ORIGINAL ARTICLE

Biological evaluation of 4,5-diarylimidazoles with hydroxamic acid appendages as novel dual mode anticancer agents

Katharina Mahal · Sebastian Schruefer · Gustav Steinemann · Franziska Rausch ·
Rainer Schobert · Bernhard Biersack · Michael Höpfner

Abstract

Purpose New (4-aryl-1-methylimidazol-5-yl)cinnamoyl-hydroxamic acids were prepared as potential dual mode anticancer agents combining the antivascular effect of the 4,5-diarylimidazole moiety and the histone deacetylases (HDAC) inhibition by the cinnamoyl hydroxamate.
Methods Their antiproliferative activity against a panel of primary cells and cancer cell lines was determined by MTT assays and their apoptosis induction by caspase-3 activation. Their ability to reduce the activity of HDAC was measured by enzymatic assays and Western blot analyses of cellular HDAC substrates. Additional effects on cancer cell migration were ascertained via immunofluorescence staining of cytoskeleton components and three-dimensional migration assays. The chorioallantoic membrane assay was used as an in vivo model to assess their antiangiogenic properties.
Results The 4-phenyl- and 4-(*p*-methoxyphenyl)-imidazole derivatives had a greater antiproliferative and apoptosis inducing effect in a variety of cancer cell lines when compared with the approved HDAC inhibitor SAHA, and most distinctly so in non-malignant human umbilical vein endothelial cells. Like SAHA, both compounds acted as pan-HDAC inhibitors. In 518A2 melanoma cells, they led to hyperacetylation of histones and of the cytoplasmic HDAC6 substrate alpha-tubulin. As a consequence, they inhibited the migration and invasion of these cells in transwell invasion assays. In keeping with its pronounced impact on endothelial cells, the 4-phenyl-imidazole derivative also inhibited the growth and sprouting of blood vessels in the chorioallantoic membrane of fertilized hen eggs.
Conclusions The 4-phenyl- and 4-(*p*-methoxyphenyl)-imidazole compounds combine the antivascular effects of 4,5-diarylimidazoles with HDAC inhibition by cinnamoyl hydroxamates and show additional antimetastatic activity. They are promising candidates for pleiotropic HDAC inhibitors.

Keywords Imidazole · Hydroxamate · HDAC inhibitor · Antiangiogenic agent · Antitumor agent · Antimetastatic activity

K. Mahal · S. Schruefer · R. Schobert · B. Biersack (✉)
Organic Chemistry Laboratory, University Bayreuth,
95440 Bayreuth, Germany
e-mail: bernhard.biersack@yahoo.com

G. Steinemann · F. Rausch · M. Höpfner (✉)
Institute of Physiology, Charité-Universitätsmedizin Berlin,
Virchowweg 6, 10117 Berlin, Germany
e-mail: michael.hoepfner@charite.de

Introduction

Histone deacetylases (HDACs) are among the most promising targets for anticancer drug development [1, 2]. The classical role of HDACs is to catalyze the N-deacetylation of lysine residues of histone proteins as part of the nucleosomes and thus to regulate gene expression. However, certain members of different HDAC classes are also responsible for the post-translational modification of non-histone substrates or proteins implicated in cell growth, cell migration or differentiation [3–8]. As a consequence, their inhibition interferes with a great number of cellular processes besides altering gene expression, by affecting protein–protein interactions, signaling transduction or protein degradation [3, 4, 6, 9].
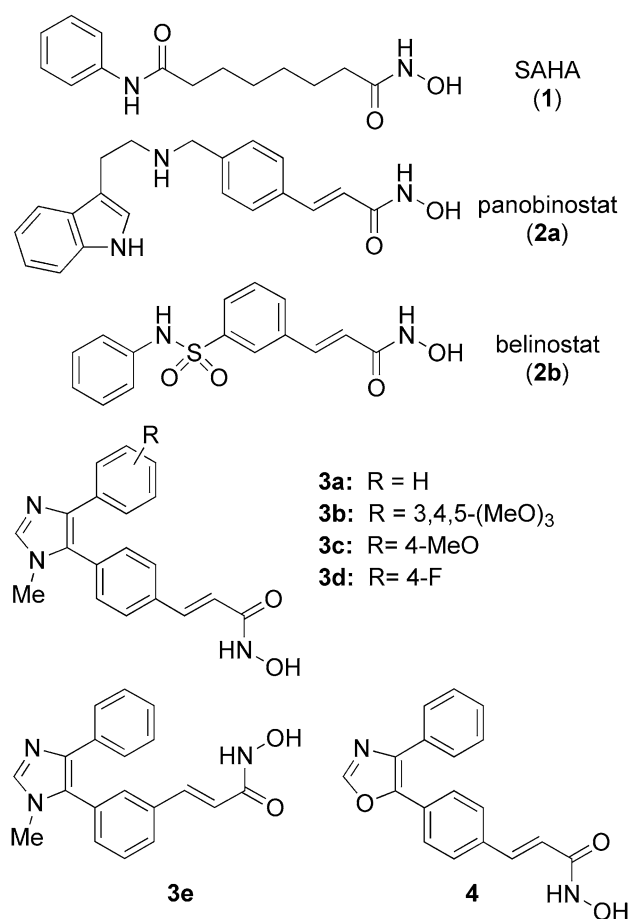
Cancer Chemother Pharmacol (2015) 75:691–700

Fig. 1 Examples of established HDAC inhibitors **1** and **2** and structures of new imidazoles **3** and oxazole **4** with hydroxamic acid appendages

These changes may eventually lead to the induction of apoptosis in cancer cells treated with HDAC inhibitors (HDACi). Hydroxamic acids are prominent (pan-) HDACi and derivatives such as SAHA (suberoylanilide hydroxamic acid, vorinostat; **1**), panobinostat (**2a**) and belinostat (**2b**) were already approved for the treatment of hematological malignancies or are in advanced clinical development (Fig. 1) [10–13]. In addition, some HDACi were also shown to exhibit antiangiogenic effects in the treatment of solid tumors in combination with other anticancer drugs [14–16]. Despite promising outcomes in clinical trials, the growing problem of resistance to HDACi necessitates their continuous development [17]. Hybrid compounds with improved anticancer activity due to synergistic combination of an inhibition of HDAC and kinase inhibition or estrogen receptor modulation were recently disclosed [18–21]. In order to enhance the efficacy of HDACi and their resilience against acquired resistance, we now attached the hydroxamic acid chelator, common to many HDACi, to a second structural motif with proven anticancer activity, the 4,5-diarylimidazole or 4,5-oxazole,

respectively. When aptly substituted such heterocyclic compounds retain the tubulin affinity as well as the vascular-disrupting and cytotoxic properties of the natural lead, the 1,2-diaryl-*cis*-stilbene combretastatin A-4, with the bonus of an increased chemical stability and water solubility [22, 23]. Derivatives of this compound class were also shown to be well tolerated by mice and orally applicable [22, 23]. A couple of 4,5-diarylimidazoles with hydroxamate appendages were reported by us recently to show antitumoral activity against hepatocellular carcinoma [24]. Herein, we report a greatly extended study comprising the synthesis of further (4-aryl-imidazole-5-yl)cinnamoylhydroxamic acids **3** and of an oxazole congener **4**, as well as an evaluation of their growth inhibitory effect on various chemosensitive and multidrug-resistant cancer cell lines, of their inhibition of HDAC, and their effect on blood vessel development in an in vivo model.

Materials and methods

Cell lines and culture conditions

The human melanoma cell line 518A2 (obtained from the department of Radiotherapy and Radiobiology, University Hospital Vienna, Austria), the human colon adenocarcinoma cell line HT-29 and the human colon carcinoma cell line HCT-116 (from University Hospital Erlangen, Germany), the MCF-7/Topo breast cancer, the KB-V1/Vbl cervix carcinoma cell line (both from the Institute of Pharmacy, University of Regensburg, Germany) and the HUVEC-derived endothelial hybrid cell line Ea.hy926 (Institute of Physiology, Charité Berlin, Germany) were grown in DMEM or RPMI (HT-29) medium, supplemented with 10 % fetal bovine serum (FBS), 1 % Antibiotic–Antimycotic solution (all from Gibco) and 250 µg/mL gentamycin (SERVA). The medium of the Ea.hy926 cells was additionally supplemented with an endothelial medium supplement (PAA). Experiments on primary human umbilical vein cells (HUVEC) were done at the Helmholtz Centre for Infection Research (Braunschweig, Germany). HUVEC were cultured in EGM-2 medium (Lonza). The human esophageal squamous carcinoma cell line Kyse-140 [25, 26] was grown in RPMI 1640 medium supplemented with 10 % FBS, the pancreatic carcinoid BON cells, which were established from a human pancreatic carcinoid tumor as a useful model to study the biology of neuroendocrine tumors in vitro were grown in a 1:1 mixture of DMEM and Ham's F-12 medium containing 10 % FCS (Biochrom, Berlin, Germany) and 1 % L-glutamine [27, 28]. Primary chicken heart fibroblasts (CHF) were explanted from 10-day-old chicken embryos and separated from other cell types for several weeks. Fibroblasts were finally grown in DMEM

(10 % FBS, 1 % Anti–Anti, 250 µg/mL gentamycin) and used before the twentieth passage. All cell lines were cultured and incubated at 37 °C, 5 % CO_2, 95 % humidified atmosphere. Only mycoplasma-free cell lines were used.

Stock solutions and drug application

The syntheses and characterization of all test compounds **3** and **4** can be found in the Electronic supplementary material (Chemistry). Stock solutions of these were prepared in DMSO at a concentration of 10 mM and stored at 4 °C. Suberoylanilide hydroxamic acid (SAHA, Vorinostat) was purchased from LC Laboratories and used without further purification as a 10 mM stock solution in DMSO. Stock solutions were diluted to the final concentration in media or ddH_2O before each experiment. In all experiments, the final DMSO concentration was <0.25 %.

Measurement of caspase-3 activity

The preparation of cell lysates and determination of caspase-3 activities was performed as previously described [29]. Caspase-3 activity was calculated from the cleavage of the fluorogenic substrate DEVD-AMC (Calbiochem-Novabiochem, Bad Soden, Germany). Cell lysate volumes normalized to their protein concentration were incubated with substrate solution (20 µg/mL caspase-3 substrate AC-DEVD-AMC in 20 mM HEPES, 10 % glycerol, 2 mM DTT, pH 7.5) for 1 h at 37 °C and a fluorescence increase after cleavage of the substrate was measured with a VersaFluor fluorometer (excitation 360 nm, emission 460 nm) from Bio-Rad. All experiments were done in triplicates. Caspase-3 activity was calculated as the mean ± S.D. with respect to DMSO controls set to 1.

HDAC activity fluorescence assay

The direct inhibition of HDAC by the new compounds was proved by means of a fluorescence-based HDAC activity assay. Visualization of HDAC activity was achieved by using short acetylated peptide substrates coupled to a precursor fluorophore which is released by trypsin cleavage only upon previous deacetylation. A commercially available nuclear extract from HeLa cells (HeLa nuclear extract, 2.0 mg/mL, Merck Millipore) containing a specific set of active HDACs with nuclear localization and a Fluor-de-Lys® substrate suitable for measuring broad-spectrum HDAC activity from cell extracts was used in this assay according to manufacturer's conditions. Briefly, 0.5 µg HeLa cell nuclear extract was mixed with SAHA, or **3a**, or **3c** (dilutions from 10 µM to 1 nM) and the Fluor-de-Lys substrate (25 µM Fluor-de-Lys®-Green substrate, Enzo Life Sciences) in a final volume of 50 µL of HDAC assay buffer

(50 mM Tris–HCl, 137 mM NaCl, 2.7 mM KCl, 1 mM $MgCl_2$, pH 8.0) in the wells of a black 96-well plate (half-area 96-well plate, µClear®, black, medium binding, greiner bio-one). The plate was incubated at 37 °C for 60 min, and the amount of deacetylated substrate was then visualized by adding 50 µL 1× developer (0.5 mg/mL trypsin, 0.1 mM EDTA in 50 mM Tris–HCl, pH 7.4) and subsequent incubation at 37 °C for 10 min. Fluorescence intensity of the degraded HDAC substrate was measured with a microplate reader (Tecan) at an emission wavelength of 535 nm (excitation at 485 nm). Blank and solvent (DMSO) controls were treated identically. The fluorescence intensity represents the relative HDAC activity within a sample with respect to DMSO controls. IC_{50} values from dose–response curves were calculated as the mean of three independent experiments ± S.D.

Detection of histone and microtubule acetylation by immunoblotting

518A2 melanoma cells (50.000 cells/well) were grown in 24-well plates and treated with vehicle (DMSO), SAHA (5 or 10 µM) or the hydroxamic acids **3a** or **3c** (5 or 10 µM) for 3, 6, 12 or 24 h. The cells were then harvested by trypsinization, and the resulting cell pellet was lysed in 100 µL 2× protein sample buffer (20 mM DTT, 2 % (w/v) SDS, 20 % (v/v) glycerol in 125 mM Tris–HCl, pH 6.8) and boiled (95 °C, 10 min). Ten microliters of the cell lysate was subjected to SDS polyacrylamide gel electrophoresis and transferred to a PVDF membrane for subsequent Western blot analysis. Drug-induced increase in histone H2B acetylation was detected by primary antibodies for acetyl-H2B (acetyl-histone H2B (Lys5) rabbit monoclonal antibody, Cell Signaling Technology). An increase in microtubule acetylation was detected by primary antibodies for alpha-tubulin (alpha-tubulin mouse monoclonal antibody, Invitrogen) and acetylated alpha-tubulin (acetyl-alpha-tubulin rabbit monoclonal antibody, Cell Signaling Technology). The membranes corresponding to two identically loaded gels were analyzed separately for alpha-tubulin and acetylated alpha-tubulin at the respective molecular weight protein band (55 kDa). Detection of beta-actin (beta-actin mouse monoclonal antibody) was used as an additional loading control. Band intensity was recorded by chemiluminescence (secondary HRP conjugates: goat antimouse-IgG-HRP conjugate, goat antirabbit-IgG-HRP conjugate, Cell Signaling Technologies; LAS-3000 imager, Fujifilm). ImageJ and Photoshop CS5 software were used for digital image processing and presentation of relevant protein bands, and contrast and brightness settings were applied uniformly to the whole images (for original blot images, see Electronic supplementary material).

Matrigel-based transwell invasion assay

The effect of the best derivatives **3a** and **3c** on the migration of highly invasive 518A2 melanoma cells [30] was assessed with a three-dimensional model for chemoattractant-stimulated tumor cell migration. It is based on modified Boyden migration chambers and implies both degradation of matrigel (trademark name) as an extracellular matrix and active movement of the cells through this basement membrane matrix [31, 32]. Quantification of invasive cells was adapted from the manufacturer's application manual (ThinCert™ application notes, greiner bio-one) with some alterations [33]. In brief, 518A2 melanoma cells were starved in serum-free DMEM overnight and harvested before seeding them into matrigel-coated (50 µL 1:1-dilution of matrigel basement membrane matrix in serum-free DMEM, 30 min at 37 °C, 5 % CO_2, 95 % humidity; BD Biosciences) ThinCert™ cell culture inserts with porous membranes (translucent PET membrane, 8 µm pore size, greiner bio-one) at a density of 2×10^4 cells in 200 µL serum-free DMEM per insert. The inserts were then placed into a 24-well plate with 600 µL DMEM containing 10 % FBS per well. Cells were incubated with DMSO (vehicle), SAHA (**1**) or **3a** or **3c** (1 µM, 36 h). Then, cells that had migrated through the insert membrane were collected and stained by incubation with 1X cell dissociation buffer (0.5 mM EDTA, 0.1 % sodium citrate in PBS, pH 7.4) containing 1 µM calcein-AM (calcein acetoxymethyl ester; non-fluorescent, cell-permeable dye) for 15 min at 37 °C. The cell suspension containing only invasive cells was transferred to the wells of a black 96-well plate, and invasive cells were quantified with a microplate reader (Tecan) by measuring the calcein fluorescence (excitation/emission wavelengths: 485/520 nm) which was eventually calculated as percentage ± S.D. of DMSO-treated control cells set to 100 %. All experiments were carried out in triplicates (for a detailed assay procedure scheme, see Electronic supplementary material, Fig. S5).

Fluorescence labeling of microtubules and actin filaments

518A2 cells (2.5×10^4/well) were seeded on glass coverslips in 24-well plates and treated with vehicle (DMSO) or the derivatives **3a** or **3c** (5 µM, 24 h). After fixation (4 % formaldehyde in PBS, 20 min), blocking and permeabilization of the cells (1 % BSA, 0.1 % Triton X-100 in PBS, 30 min), microtubules were visualized by incubation of the coverslips with a primary antibody against alpha-tubulin (antialpha-tubulin, mouse monoclonal antibody, clone no. TU-01, 1 h at 37 °C) followed by incubation with a secondary antibody conjugated to the DyLight550 fluorescence dye (goat antimouse-IgG-DyLight550 conjugate, Thermo Scientific/Pierce, 1 h at rt in the dark). Filamentous actin

(F-actin) was stained by incubation of the coverslips with 1 U AlexaFluor®-488-conjugated phalloidin (Invitrogen) for 1 h at rt. The coverslips were mounted in Mowiol 4-88-based mounting medium containing 2.5 % (w/v) DABCO and 1 µg/mL DAPI (4′,6-diamidino-2-phenyl-indole) for counterstaining the nuclei. Cytoskeletal components were documented by fluorescence microscopy (ZEISS Axio Imager.A1; 400-fold magnification).

Chorioallantoic membrane (CAM) assay with fertilized chicken eggs

White leghorn chicken eggs (SPF eggs, VALO Biomedia) were incubated (37 °C, 50–60 % humidity) until day 6 after fertilization and opened by cutting a window of 2–3 cm diameter into the pole end of the eggshell. Rings of silicon foil (8 mm diameter) were placed on the developing vessels within the CAM followed by further incubation for 24 h. A total amount of 20 nmol (40 µL of 50 µM dilutions in ddH$_2$O) SAHA or the endothelial cell-selective derivative **3a** were applied directly onto the CAM and alterations in the blood vessel organization in comparison to control eggs (DMSO) were documented after 0-h and 24-h post-application with a stereomicroscope (60-fold magnification, Traveller) [34].

Data analysis and statistical analysis

The experimental results presented in the figures are representative of three or more independent observations. The data are presented as the mean values ± SD. Analysis of statistical significance was done by two-sample Student's t tests with XLSTAT. P values < 0.05 were considered to be statistically significant. ImageJ or Photoshop CS5 software was used for digital processing of original pictures and figure preparation (for additional information on image processing, see Electronic supplementary material).

Results and discussion

Tumor cell growth inhibition and apoptosis induction

The compounds **3a–e** and **4** were tested for their antiproliferative activity against a panel of cancer and endothelial cells of different origin and with different characteristics (Table 1). To assess a compound selectivity for rapidly dividing cancer over non-malignant cells, we also included non-malignant primary chicken fibroblasts.

The derivatives **3a**, **3c**, **3d** and **3e** were active with IC$_{50}$ values in the low micromolar range (<3 µM). On average, the anisyl derivative **3c** was the most active compound of this series in the tested cell lines which included

Table 1 Inhibitory concentrations[a] IC$_{50}$ [μM] of SAHA (**1**) and compounds **3a-e** and **4** when applied to various cancer and endothelial cells and non-malignant fibroblasts

	SAHA (**1**)	**3a**	**3b**	**3c**	**3d**	**3e**	**4**
518A2[b]	18.7 ± 3.1	13.1 ± 0.9	>50	10.2 ± 0.3	11.1 ± 2.0	n.d.	18.6 ± 2.5
518A2[c]	1.8 ± 0.1	2.8 ± 0.6	20.8 ± 3.0	1.5 ± 0.1	2.0 ± 0.5	2.3 ± 0.1	10.2 ± 0.1
HCT-116[c]	0.9 ± 0.1	0.8 ± 0.1	7.5 ± 3.0	0.9 ± 0.1	1.0 ± 0.1	1.1 ± 0.03	5.5 ± 1.4
HT-29[b]	1.9 ± 0.3	0.5 ± 0.1	n.d.	0.4 ± 0.1	0.3 ± 0.1	n.d.	n.d.
HT-29[c]	1.8 ± 0.1	1.2 ± 0.1	7.9 ± 1.0	0.7 ± 0.1	1.5 ± 0.1	2.5 ± 0.6	8.3 ± 0.3
MCF-7/Topo[c]	13.5 ± 0.7	15.3 ± 1.3	n.d.	10.0 ± 0.9	17.4 ± 1.0	18.0 ± 1.0	8.6 ± 1.4
KB-V1/Vbl[c]	13.1 ± 0.8	5.0 ± 0.8	n.d.	8.3 ± 1.9	5.5 ± 0.4	18.2 ± 2.6	8.0 ± 0.4
Panc-1[c]	3.8 ± 1.2	1.1 ± 0.1	8.7 ± 1.0	0.9 ± 0.1	1.7 ± 0.9	2.0 ± 0.1	2.4 ± 0.2
Ea.hy926[c]	1.9 ± 0.2	0.2 ± 0.1	n.d.	0.9 ± 0.1	2.3 ± 0.3	n.d.	10.0 ± 2.6
HUVEC[c]	7.7 ± 0.1	0.6 ± 0.03	n.d.	0.8 ± 0.1	n.d.	n.d.	n.d.
CHF[c]	89.4 ± 9.8	>150 μM	n.d.	>150 μM	>150 μM	n.d.	n.d.
BON[d]	>10 μM	n.d.	n.d.	1.1 ± 0.1	2.3 ± 0.6	n.d.	n.d.
BON[e]	2.2 ± 0.5			1.3 ± 0.2	3.6 ± 0.7		
Kyse-140[d]	>10 μM	n.d.	n.d.	4.6 ± 1.1	3.5 ± 1.0	n.d.	n.d.
Kyse-140[e]	3.1 ± 0.6			1.7 ± 0.1	6.1 ± 1.5		

Human cancer cell lines: 518A2 melanoma, HCT-116 colon, HT-29 colon, MCF-7/Topo breast, KB-V1/Vbl cervix, Panc-1 pancreas, neuroendocrinic carcinoid BON (pancreas) and Kyse-140 esophageal squamous cell carcinoma. Endothelial cells: hybrid cell line Ea.hy926 and primary cells (HUVEC). Non-malignant chicken heart fibroblasts: CHF. Values represent means of at least three independent assays ± S.D

nd not determined

[a] Values derived from concentration–response curves obtained by measuring the percentage of vital cells relative to vehicle-treated controls after 24-h[b] or 72-h[c] incubation using an MTT assay, or after 24-h[d] or 48-h[e] incubation using crystal violet staining

highly invasive 518A2 melanoma and p53-wild type, ras-mutated HCT-116 colon carcinoma cells, as well as the multidrug-resistant cell lines HT-29 colon, MCF-7/Topo mammary, KB-V1/Vbl cervix, and Panc-1 pancreas carcinomas. Compound **3c** displayed a sub-micromolar IC$_{50}$ value of 0.68 μM in the multidrug-resistant HT-29 colon cancer cells, while it was active against the drug-sensitive 518A2 melanoma cells only at an IC$_{50}$ of 1.45 μM. The *para*-fluoro substituted congener **3d** was also among the three best performing derivatives. Interestingly, HT-29 cells responded very well upon short time incubation with **3a**, **3c** and **3d** [IC$_{50}$ (24 h) < 1 μM], whereas only **3c** was similarly active upon 72-h incubation of these cells. In general, **3a** and **3c** displayed a higher cytotoxicity against all cell lines than SAHA which was used as a positive, clinically established control. In contrast, low activities were observed for the 3,4,5-trimethoxyphenyl derivative **3b** and for **4**, the oxazole analog of the well-performing imidazole **3a**. These results suggest that high antiproliferative activity will arise only for *N*-methyl-imidazoles bearing a mono-substituted 4-phenyl ring as in **3c**. Furthermore, we observed a pronounced selectivity of **3a** for both the endothelial cell line Ea.hy926 and primary endothelial cells (HUVEC) with IC$_{50}$ (72 h) values only a tenth of those of SAHA. Interestingly, the growth of primary fibroblasts was hardly reduced by high concentrations of **3a** or the most active compound **3c**. In contrast, SAHA affected these cells at the lowest IC$_{50}$ (72 h) value.

The inhibition of HDACs is a particularly attractive approach for the treatment of advanced neuroendocrine tumors (NET) since NET cells had responded well to established HDAC inhibitors like trichostatin A, sodium butyrate and MS-275 [35]. Epigenetic modification of esophageal squamous cell carcinomas (ESCC) likewise led to tumor-suppressive effects [36]. Hence, the compounds **3c** and **3d** were also tested on human carcinoid BON cells obtained from a rare pancreatic neuroendocrine tumor and in Kyse-140 esophageal squamous cell carcinoma cells. Compound **3c** was more efficacious than **3d** against both cancer cell lines with IC$_{50}$ (48 h) values between 1 and 2 μM.

3c and to a lesser extent also **3d** induced apoptosis in highly migratory 518A2 melanoma as well as in BON and Kyse-140 cells apparent from an increase of the caspase-3 activity after exposure to 2.5 or 10 μM concentrations for 24 h (Fig. 2). These findings are in line with the respective results of the growth inhibition studies. The values for equimolar concentrations of SAHA were in the same range with exception of those for Kyse-140 cells where **3c** clearly was more efficient in activating caspase-3.
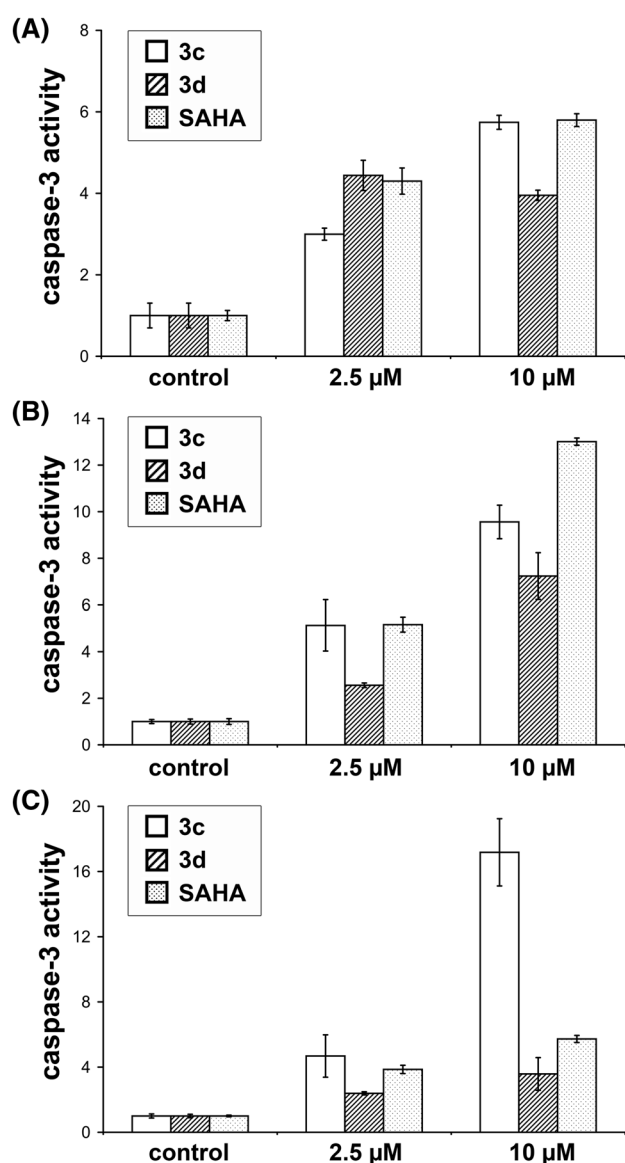
(A)

(B)

(C)

Fig. 2 Induction of caspase-3 activity. Caspase-3 activity upon 24 h exposure to SAHA (**1**) or the hydroxamic acids **3c** or **3d** in a 518A2 melanoma, b human carcinoid BON (pancreatic neuroendocrine tumor), and c Kyse-140 esophageal squamous cell carcinoma cells. Basal caspase-3 activity of vehicle-treated controls was set to 1. *Data* represent the mean ± S.D. of three independent experiments

Determination of HDAC inhibition via activity assays and detection of histone H2B and alpha-tubulin acetylation

To assess a direct inhibition of HDACs, we tested the compounds **3a** and **3c** on commercially available HeLa cell nuclear extract containing a specific set of active HDACs [9]. The resulting IC_{50} value calculated for **3a** (0.23 ± 0.01 μM) is similar to that of SAHA (0.23 ± 0.03 μM). Interestingly, the more cytotoxic compound **3c** inhibited HDAC activity in the extract only with
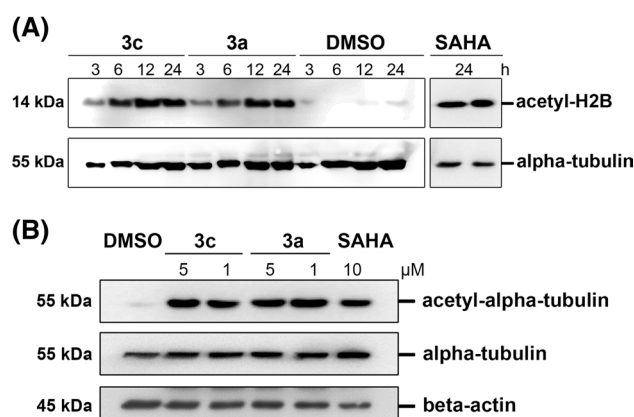

(A)

(B)

Fig. 3 Effects on histone H2B and alpha-tubulin acetylation. Increase of protein acetylation in 518A2 melanoma cells after treatment with **3a** or **3c**. a Time-dependent increase of histone H2B acetylation after exposure to 5 μM **3a** or **3b** for 3, 6, 12 and 24 h, or to SAHA (10 and 5 μM, 24 h) as detected by immunoblotting; alpha-tubulin: loading control. b Increase in microtubule (alpha-tubulin) acetylation after exposure to indicated concentrations of **3a**, **3c**, or SAHA for 24 h. Equal sample volumes were subjected to gel electrophoresis and immunoblotting for acetylated or total alpha-tubulin (55 kDa); beta-actin: loading control

a fivefold higher IC_{50} value of 1.08 ± 0.1 μM (for IC_{50} values, see Table S1 in the Electronic supplementary material).

The actual HDAC inhibition by the new compounds was additionally assessed by immunodetection of the increased portion of acetylated histone H2B which is part of the nucleosome. Exposure of 518A2 cells to 5 μM of **3a** or **3c** led to strongly increased H2B acetylation after only 3 h (Fig. 3a) and to a general increase in histone acetylation (*cf.* Electronic supplementary material, Fig. S1) when compared to DMSO-treated controls. This effect is restricted to the imidazoles with hydroxamic acid appendages and did not occur when cells were treated with the recently described, combretastatin A-4-derived imidazoles lacking hydroxamate residues (*cf.* Electronic supplementary material, Fig. S3) [23]. Furthermore, HDAC activity is not limited to the deacetylation of histones. Certain HDAC enzymes are not located in the nucleus at all. HDAC6, for instance, is occurring exclusively in the cytoplasm where it associates with microtubules. It was shown that HDAC6 removes acetyl groups from lysine residues of alpha-tubulin [37, 38]. In order to assess the HDAC specificity of the new hydroxamates **3a** and **3c,** we investigated the level of acetylated lysines of alpha-tubulin proteins in treated 518A2 melanoma cells. Both compounds led to significantly enhanced levels of acetylated tubulin (Fig. 3b). While **3a** caused levels of acetylated lysine in tubulin similarly to SAHA, **3c** was more effective in eliciting acetylated tubulin than SAHA, even at the lower concentration of 5 μM. We assume a greater inhibition of HDAC6 by compound **3c** to be responsible for this

Fig. 4 Effects of **3a** or **3c** on migration and cytoskeleton of 518A2 melanoma cells. **a** Invasive 518A2 cells (%) after exposure to non-toxic concentrations of SAHA, **3c** or **3a** (1 μM, 36 h) or vehicle (DMSO). *Data* represent the mean of the calcein fluorescence of cells migrated through matrigel-coated cell culture inserts in transwell migration assays ± S.D. *Asterisks* indicate statistically significant differences ($P = 0.003$ for vehicle versus **3c**, $P = 0.006$ for SAHA versus **3c**, two-tailed Student's *t* test). **b** Fluorescence staining of microtubules (alpha-tubulin, merge: *red*) and filamentous actin (F-actin, merge: *green*) in 518A2 cells after incubation with vehicle (DMSO) or the derivatives **3a**, **3c** (5 μM, 24 h). Nuclei counterstained with DAPI (*blue*). *Scale bar* 100 μm
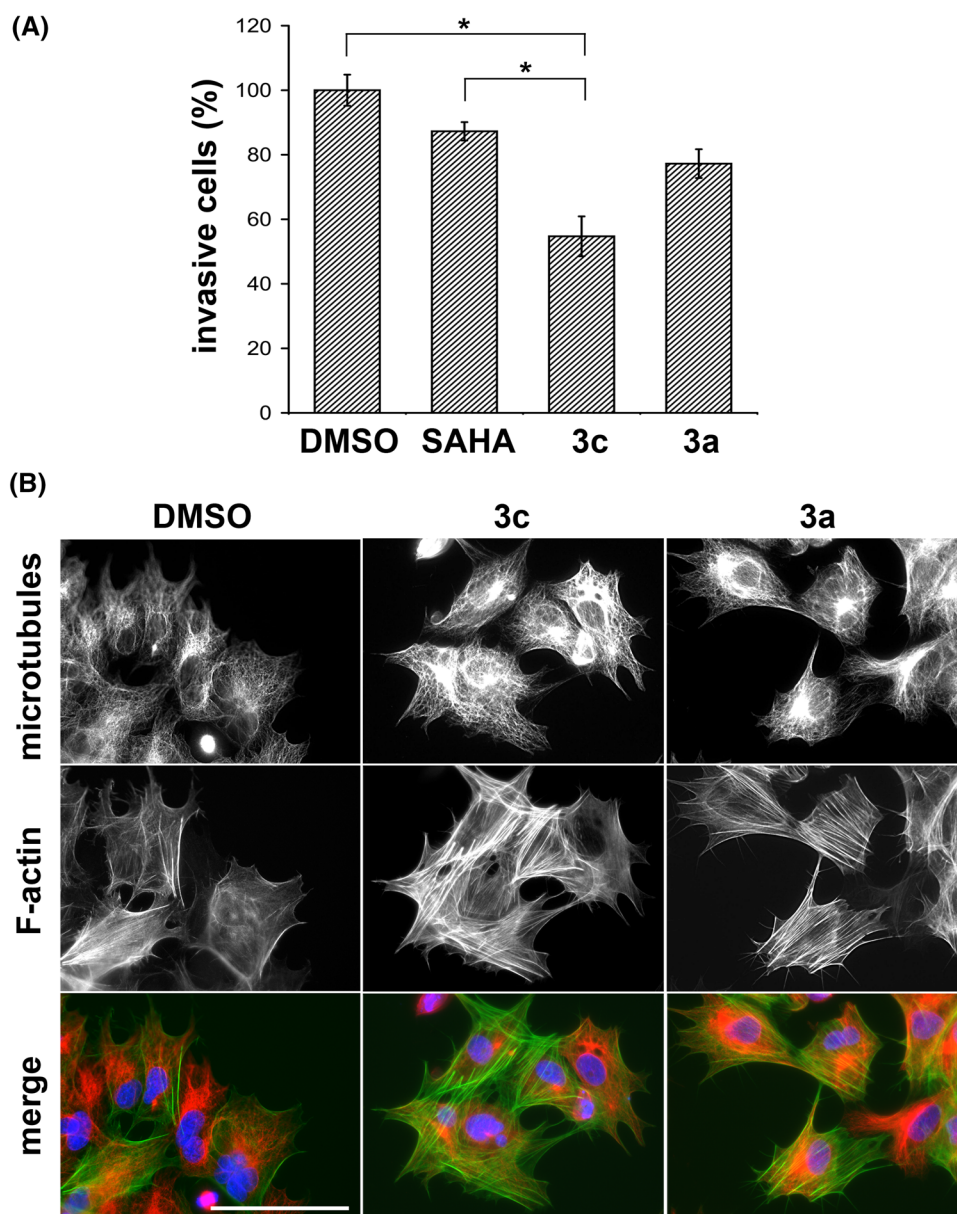

increase in acetylated microtubules in the 518A2 melanoma cells [37–39].

Migration and microfilament behavior of treated 518A2 melanoma cells

Like intact microtubules, a functional actin cytoskeleton is essential for directed cell migration by enabling highly dynamic structures such as membrane ruffles or lamellipodia [40]. As the actin cytoskeleton can be affected by HDAC inhibition in several ways [4, 41, 42], we investigated the effect of the derivatives **3a** and **3c** on the migration and the microfilament behavior of 518A2 melanoma cells (Fig. 4). In a three-dimensional transwell invasion assay, starved cells migrated to a lower compartment of a modified Boyden two-chamber system that is baited with fetal bovine serum as a chemoattractant and separated by a porous membrane and a matrigel layer as a surrogate for the extracellular matrix or the basement membrane of a microtumor. We found that non-toxic concentrations (1 μM, 36 h) of **3c** reduced the number of cells capable of migrating through matrigel-coated cell culture inserts to 55 % (Fig. 4a). Equimolar concentrations of SAHA reduced the directed cell invasion only to about 87 %. This pronounced antimigratory effect of compounds **3a** and **3c** might be a consequence of their interference with cytoskeletal dynamics via HDAC6 inhibition which leads to compacted microtubules and actin stress fiber formation (Fig. 4b). These structures likely lack the dynamic turnover that is essential of active migration [43].

Fig. 5 Antiangiogenic effects of SAHA and **3a** (20 nmol) in a chorioallantoic membrane (CAM) assay with fertilized chicken eggs. Pictures (60-fold magnification) were taken 24 h after topical application onto the CAM of eggs at day 6 and 7 post-fertilization. *Pictures* are representative of at least three independent experiments
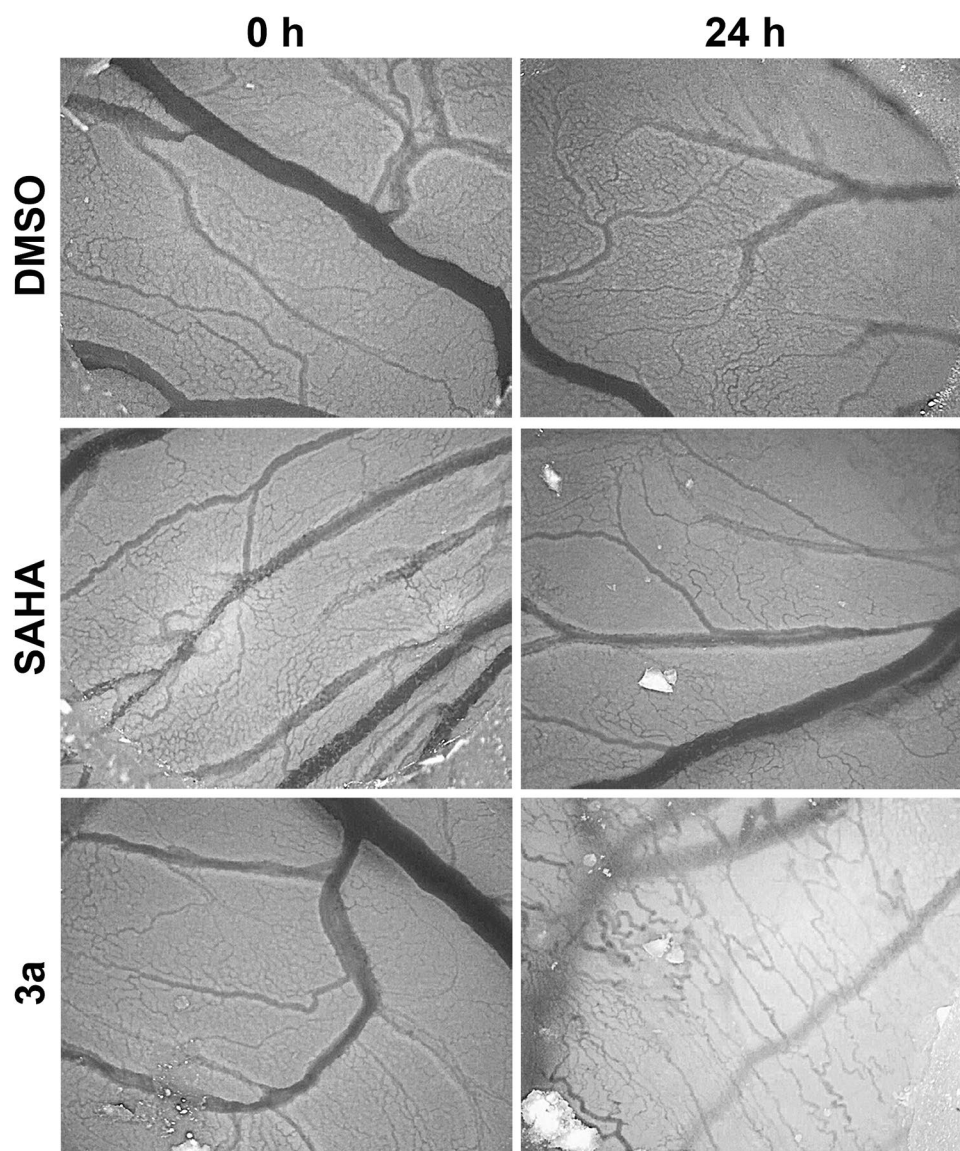
Antiangiogenic activity in vivo using the CAM assay

Furthermore, we tested the impact of the endothelial cell-selective derivative **3a** on blood vessel development in the chorioallantoic membrane (CAM) of fertilized chicken eggs (Fig. 5). The marginal antiangiogenic effect of SAHA was surpassed by that of **3a** which induced significant alterations of the vascular organization and reduced the sprouting of new blood vessels. A lesser effect, similar to that of SAHA, was observed for **3c** (not shown). A dose of 20 nmol of either **3a** or **3c** topically applied onto the CAM did not affect the vitality and development of the chicken embryos. Hence, both compounds **3a** and **3c** are at least as good antiangiogenic agents as SAHA or other HDACi described as such in the literature [14–16]. Mechanistically, this antiangiogenic effect of **3a** and **3c** might involve aberrant VEGF/VEGFR (vascular endothelial growth factor

receptor) or the destabilization of the pro-angiogenic transcription factor HIF-1alpha [4, 44, 45] as has been discussed for SAHA. However, the exact mechanism and the contribution of conceivable signaling pathways remain to be elucidated.

Conclusions

Our initial objective to combine the antivascular effect of 4,5-diarylimidazoles with the HDAC inhibition cum downstream anticancer effects of cinnamoylhydroxamic acids was largely met. The new (4-aryl-1-methylimidazol-5-yl)cinnamoylhydroxamic acids **3a** and **3c** were more strongly antiproliferative and apoptosis inducing in various cancer and endothelial cells (Ea.hy926 and HUVEC) than the established HDAC inhibitor SAHA

(**1**), while non-malignant fibroblasts were hardly affected. The pronounced cytotoxicity of **3a** against dividing endothelial cells correlates with its strong antiangiogenic activity in the CAM model which exceeds that of SAHA by far. Like SAHA, the new conjugates are pan-HDAC inhibitors which led to an accumulation of hyperacetylated histones and alpha-tubulin in 518A2 melanoma cells, with the consequence of impaired cell migration and invasion.

In combination, the new imidazole hydroxamate conjugates are multimodal anticancer agents that should act on primary tumors of various entities, in particular well vascularized ones, and at the same time should impede the absconding of individual tumor cells and their metastatic spread. Against the background of good tolerance of the parent 4,5-diarylimidazoles in previous animal studies, we expect the new hydroxamate derivatives **3** to be suitable for in vivo xenograft studies, too. All the more so since they are well soluble in water, chemically stable, and very likely orally applicable. Finally, it should be noted that there is ample opportunity for fine-tuning mechanistic subtleties and optimizing the overall efficacy of the new antivascular HDACi of type **3** by adjusting the substituents and the three aromatic rings.

Conflict of interest None.

References

1. Nebbioso A, Carafa V, Benedetti R, Altucci L (2012) Trials with "epigenetic" drugs: an update. Mol Oncol 6:657–682. doi:10.1016/j.molonc.2012.09.004
2. New M, Olzscha H, La Thangue NB (2012) HDAC inhibitor-based therapies: can we interpret the code? Mol Oncol 6:637–656. doi:10.1016/j.molonc.2012.09.003
3. Glozak MA, Seto E (2007) Histone deacetylases and cancer. Oncogene 26:5420–5432. doi:10.1038/sj.onc.1210610
4. Aldana-Masangkay GI, Sakamoto KM (2011) The role of HDAC6 in cancer. J Biomed Biotechnol 2011:1–10. doi:10.1155/2011/875824
5. Vidali G, Boffa LC, Bradbury EM, Allfrey VG (1978) Butyrate suppression of histone deacetylation leads to accumulation of multiacetylated forms of histones H3 and H4 and increased DNase I sensitivity of the associated DNA sequences. Proc Natl Acad Sci 75:2239–2243
6. Minucci S, Pelicci PG (2006) Histone deacetylase inhibitors and the promise of epigenetic (and more) treatments for cancer. Nat Rev Cancer 6:38–51. doi:10.1038/nrc1779
7. Paris M, Porcelloni M, Binaschi M, Fattori D (2008) Histone deacetylase inhibitors: from bench to clinic. J Med Chem 51:1505–1529. doi:10.1021/jm7011408
8. Mai A, Altucci L (2009) Epi-drugs to fight cancer: from chemistry to cancer treatment, the road ahead. Int J Biochem Cell Biol 41:199–213. doi:10.1016/j.biocel.2008.08.020
9. Dokmanovic M, Clarke C, Marks PA (2007) Histone deacetylase inhibitors: overview and perspectives. Mol Cancer Res 5:981–989. doi:10.1158/1541-7786.MCR-07-0324
10. Richon VM, Emiliani S, Verdin E et al (1998) A class of hybrid polar inducers of transformed cell differentiation inhibits histone deacetylases. Proc Natl Acad Sci 95:3003–3007
11. Marks PA (2007) Discovery and development of SAHA as an anticancer agent. Oncogene 26:1351–1356. doi:10.1038/sj.onc.1210204
12. Maiso P, Carvajal-Vergara X, Ocio EM et al (2006) The histone deacetylase inhibitor LBH589 is a potent antimyeloma agent that overcomes drug resistance. Cancer Res 66:5781–5789
13. Plumb JA, Finn PW, Williams RJ et al (2003) Pharmacodynamic response and inhibition of growth of human tumor xenografts by the novel histone deacetylase inhibitor PXD101. Mol Cancer Ther 2:721–728
14. Ellis L, Hammers H, Pili R (2009) Targeting tumor angiogenesis with histone deacetylase inhibitors. Cancer Lett 280:145–153. doi:10.1016/j.canlet.2008.11.012
15. Kim H-J, Bae S-C (2011) Histone deacetylase inhibitors: molecular mechanisms of action and clinical trials as anti-cancer drugs. Am J Transl Res 3:166
16. Qian DZ (2006) Targeting tumor angiogenesis with histone deacetylase inhibitors: the hydroxamic acid derivative LBH589. Clin Cancer Res 12:634–642. doi:10.1158/1078-0432.CCR-05-1132
17. Fantin VR, Richon VM (2007) Mechanisms of resistance to histone deacetylase inhibitors and their therapeutic implications. Clin Cancer Res 13:7237–7242. doi:10.1158/1078-0432.CCR-07-2114
18. Wang J, Pursell NW, Samson MES et al (2013) Potential advantages of CUDC-101, a multitargeted HDAC, EGFR, and HER2 inhibitor, in treating drug resistance and preventing cancer cell migration and invasion. Mol Cancer Ther 12:925–936. doi:10.1158/1535-7163.MCT-12-1045
19. Mahboobi S, Dove S, Sellmer A et al (2009) Design of chimeric histone deacetylase- and tyrosine kinase-inhibitors: a series of imatinib hybrides as potent inhibitors of wild-type and mutant BCR-ABL, PDGF-Rβ, and histone deacetylases. J Med Chem 52:2265–2279. doi:10.1021/jm800988r
20. Gryder BE, Rood MK, Johnson KA et al (2013) Histone deacetylase inhibitors equipped with estrogen receptor modulation activity. J Med Chem 56:5782–5796. doi:10.1021/jm400467w
21. Guerrant W, Patil V, Canzoneri JC et al (2013) Dual-acting histone deacetylase-topoisomerase I inhibitors. Bioorg Med Chem Lett 23:3283–3287. doi:10.1016/j.bmcl.2013.03.108
22. Biersack B, Effenberger K, Schobert R, Ocker M (2010) Oxazole-bridged combretastatin a analogues with improved anticancer properties. ChemMedChem 5:420–427. doi:10.1002/cmdc.200900477
23. Schobert R, Biersack B, Dietrich A et al (2010) 4-(3-Halo/amino-4,5-dimethoxyphenyl)-5-aryloxazoles and -N-methylimidazoles that are cytotoxic against combretastatin a resistant tumor cells and vascular disrupting in a cisplatin resistant germ cell tumor model. J Med Chem 53:6595–6602. doi:10.1021/jm100345r
24. Di Fazio P, Lingelbach S, Schobert R, Biersack B (2014) 4,5-Diaryl imidazoles with hydroxamic acid appendages as anti-hepatoma agents. Invest New Drugs. doi:10.1007/s10637-014-0188-0
25. Shimada Y, Imamura M, Wagata T et al (1992) Characterization of 21 newly established esophageal cancer cell lines. Cancer 69:277–284
26. Sutter AP, Höpfner M, Huether A et al (2006) Targeting the epidermal growth factor receptor by erlotinib (Tarceva™) for the treatment of esophageal cancer. Int J Cancer 118:1814–1822. doi:10.1002/ijc.21512
27. Evers BM, Ishizuka J, Townsend CM, Thompson JC (1994) The human carcinoid cell line, BON: a model system for the study of carcinoid tumors. Ann N Y Acad Sci 733:393–406. doi:10.1111/j.1749-6632.1994.tb17289.x

28. Gloesenkamp CR, Nitzsche B, Ocker M et al (2011) AKT inhibition by triciribine alone or as combination therapy for growth control of gastroenteropancreatic neuroendocrine tumors. Int J Oncol 40:876–888. doi:10.3892/ijo.2011.1256

29. Gloesenkamp C, Nitzsche B, Lim AR et al (2012) Heat shock protein 90 is a promising target for effective growth inhibition of gastrointestinal neuroendocrine tumors. Int J Oncol 40:1659–1667. doi:10.3892/ijo.2012.1328

30. Hofmann UB, Houben R, Bröcker E-B, Becker JC (2005) Role of matrix metalloproteinases in melanoma cell invasion. Biochimie 87:307–314. doi:10.1016/j.biochi.2005.01.013

31. Boyden S (1962) The chemotactic effect of mixtures of antibody and antigen on polymorphonuclear leucocytes. J Exp Med 115:453–466

32. Entschladen F, Drell TL, Lang K et al (2005) Analysis methods of human cell migration. Exp Cell Res 307:418–426. doi:10.1016/j.yexcr.2005.03.029

33. Albini A, Iwamoto Y, Kleinman HK et al (1987) A rapid in vitro assay for quantitating the invasive potential of tumor cells. Cancer Res 47:3239–3245

34. Nitzsche B, Gloesenkamp C, Schrader M et al (2010) Novel compounds with antiangiogenic and antiproliferative potency for growth control of testicular germ cell tumours. Br J Cancer 103:18–28. doi:10.1038/sj.bjc.6605725

35. Baradari V, Huether A, Hopfner M et al (2006) Antiproliferative and proapoptotic effects of histone deacetylase inhibitors on gastrointestinal neuroendocrine tumor cells. Endocr Relat Cancer 13:1237–1250. doi:10.1677/erc.1.01249

36. Kim MS, Yamashita K, Baek JH et al (2006) N-methyl-D-aspartate receptor type 2B is epigenetically inactivated and exhibits tumor-suppressive activity in human esophageal cancer. Cancer Res 66:3409–3418

37. Zhang Y, Li N, Caron C et al (2003) HDAC-6 interacts with and deacetylates tubulin and microtubules in vivo. EMBO J 22:1168–1179

38. Hubbert C, Guardiola A, Shao R et al (2002) HDAC6 is a microtubule-associated deacetylase. Nature 417:455–458. doi:10.1038/417455a

39. Matsuyama A, Shimazu T, Sumida Y et al (2002) In vivo destabilization of dynamic microtubules by HDAC6-mediated deacetylation. EMBO J 21:6820–6831

40. Sadoul K, Wang J, Diagouraga B, Khochbin S (2011) The tale of protein lysine acetylation in the cytoplasm. J Biomed Biotechnol 2011:1–15. doi:10.1155/2011/970382

41. Kim SC, Sprung R, Chen Y et al (2006) Substrate and functional diversity of lysine acetylation revealed by a proteomics survey. Mol Cell 23:607–618. doi:10.1016/j.molcel.2006.06.026

42. Zhang X, Yuan Z, Zhang Y et al (2007) HDAC6 modulates cell motility by altering the acetylation level of cortactin. Mol Cell 27:197–213. doi:10.1016/j.molcel.2007.05.033

43. Friedl P, Wolf K (2003) Tumour-cell invasion and migration: diversity and escape mechanisms. Nat Rev Cancer 3:362–374. doi:10.1038/nrc1075

44. Deroanne CF, Bonjean C, Servotte S et al (2002) Histone deacetylases inhibitors as anti-angiogenic agents altering vascular endothelial growth factor signaling. Oncogene 21:427–436

45. Jeong J-W, Bae M-K, Ahn M-Y et al (2002) Regulation and destabilization of HIF-1α by ARD1-mediated acetylation. Cell 111:709–720